Functional Interactions of Ribosomal Intersubunit Bridges in *Saccharomyces cerevisiae*

Tiina Tamm,[1] Ivan Kisly, and Jaanus Remme
Department of Molecular Biology, Institute of Molecular and Cell Biology, University of Tartu, 51010 Estonia
ORCID ID: 0000-0001-9943-2097 (T.T.)

ABSTRACT Ribosomes of Archaea and Eukarya share higher homology with each other than with bacterial ribosomes. For example, there is a set of 35 r-proteins that are specific only for archaeal and eukaryotic ribosomes. Three of these proteins—eL19, eL24, and eL41—participate in interactions between ribosomal subunits. The eukaryote-specific extensions of r-proteins eL19 and eL24 form two intersubunit bridges eB12 and eB13, which are present only in eukaryotic ribosomes. The third r-protein, eL41, forms bridge eB14. Notably, eL41 is found in all eukaryotes but only in some Archaea. It has been shown that bridges eB12 and eB13 are needed for efficient translation, while r-protein eL41 plays a minor role in ribosome function. Here, the functional interactions between intersubunit bridges were studied using budding yeast strains lacking different combinations of the abovementioned bridges/proteins. The growth phenotypes, levels of *in vivo* translation, ribosome–polysome profiles, and *in vitro* association of ribosomal subunits were analyzed. The results show a genetic interaction between r-protein eL41 and the eB12 bridge-forming region of eL19, and between r-proteins eL41 and eL24. It was possible to construct viable yeast strains with Archaea-like ribosomes lacking two or three eukaryote-specific bridges. These strains display slow growth and a poor translation phenotype. In addition, bridges eB12 and eB13 appear to cooperate during ribosome subunit association. These results indicate that nonessential structural elements of r-proteins become highly important in the context of disturbed subunit interactions. Therefore, eukaryote-specific bridges may contribute to the evolutionary success of eukaryotic translation machinery.

KEYWORDS *Saccharomyces cerevisiae*; ribosomal proteins; protein synthesis; protein domains; intersubunit bridges

RIBOSOMES are large ribonucleoprotein complexes that translate the genetic information encoded in messenger RNA (mRNA) into proteins. In all living cells, ribosomes consist of two unequal subunits: a small (SSU; 30S in prokaryotes and 40S in eukaryotes) and a large (LSU; 50S in prokaryotes and 60S in eukaryotes) subunit. These subunits join together to form a functional ribosome (70S in prokaryotes and 80S in eukaryotes). As the ribosomes are the central sites for protein synthesis, many key components of the ribosomes are conserved across the three domains of life: Bacteria, Archaea, and Eukarya. It has become evident that ribosomes share a common structural core, comprising 33 conserved ribosomal proteins (r-proteins) and ~4400 RNA nucleotides (Melnikov *et al.* 2012; Ban *et al.* 2014). In addition to the core structure, the ribosomes from different life domains contain their own set of specific elements (Melnikov *et al.* 2012). These elements are domain-specific proteins, extensions of conserved proteins, and expansion segments of ribosomal RNA (rRNA). The eukaryotic ribosome is considerably larger and more complex than the bacterial and archaeal ribosomes (Ben-Shem *et al.* 2011; Anger *et al.* 2013). It contains ~80 different proteins (Ban *et al.* 2014). In addition to the universally conserved r-proteins that belong to the ribosomal common core, eukaryotic ribosomes contain r-proteins that are present only in Eukarya (Ben-Shem *et al.* 2011; Anger *et al.* 2013). For example, the 80S ribosome of *Saccharomyces cerevisiae* contains 11 Eukarya-specific r-proteins. In addition, eukaryotic ribosomes share 35 r-proteins with archaeal ribosomes. Many of these r-proteins have evolved eukaryote-specific extensions, and are mainly located on the solvent-exposed surfaces of the SSU and LSU (Klinge *et al.* 2012). This study focuses on three LSU r-proteins: eL19, eL24, and eL41. These proteins are not present in the bacterial ribosome. The r-proteins eL19 and

doi: https://doi.org/10.1534/genetics.119.302777
Manuscript received June 13, 2019; accepted for publication October 22, 2019; published Early Online October 24, 2019.
Supplemental material available at figshare: https://doi.org/10.25386/genetics.9995402.
[1]Corresponding author: Institute of Molecular and Cell Biology, University of Tartu, Riia 23, Tartu 51010, Estonia. E-mail: ttamm@ut.ee

eL24 contain the domains that are conserved in archaeal and eukaryotic ribosomes. In addition, they have eukaryote-specific extensions that carry out specific functions (Kisly *et al.* 2016, 2019). eL41 is the smallest r-protein in the ribosomes (Planta and Mager 1998). Interestingly, eL41 is present in all eukaryotic ribosomes and in some, but not all, archaeal ribosomes (Lecompte *et al.* 2002).

During translation initiation, two subunits associate to form functional 80S ribosomes that will continue with protein synthesis. The intersubunit contacts, called intersubunit bridges, play an important role during the formation of 80S particles. Based on structural studies of bacterial and eukaryotic ribosomes, these contacts are divided into conserved contacts (present in both) and domain-specific bridges (Yusupov *et al.* 2001; Ben-Shem *et al.* 2011). In the 80S ribosome, the conserved bridges are located close to the ribosomal functional centers and consist of rRNA–rRNA, protein–rRNA, and protein–protein-type contacts. The eukaryote-specific bridges are mainly placed at the periphery of the subunit interface and are formed by protein–rRNA and protein–protein interactions. Two of the eukaryote-specific bridges, namely eB12 and eB13, are characterized by distinctive features. Both bridges are formed by long extensions of the LSU r-proteins eL19 and eL24, which reach the body, right foot, and h44 of the SSU from the solvent side (Figure 1A).

The main component of the eB12 bridge, r-protein eL19, contains three structural domains: an N-terminal globular domain, a middle region, and a long C-terminal α-helical domain (Supplemental Material, Figure S1A) (Ben-Shem *et al.* 2011). The globular domain and middle region are embedded in the 25S rRNA of the LSU, and are essential during ribosome biogenesis (Pöll *et al.* 2009; Kisly *et al.* 2016). The C-terminal α-helical domain extends out from the LSU and forms the eB12 bridge through interactions with the eukaryote-specific rRNA expansion segment 6 (ES6S) of 18S rRNA (Figure 1B) (Ben-Shem *et al.* 2011). Additional stabilizing interactions between eL19 and the SSU r-proteins eS7 or uS17 are also involved, depending on the rotational state of the ribosome. Mutational analysis of eL19 revealed that the functional integrity of the eB12 bridge depends on the protein–rRNA contacts (Kisly *et al.* 2016). Biochemical analysis determined that bridge eB12 is essential for the formation of 80S ribosomes *in vitro* (Kisly *et al.* 2016).

The r-protein eL19 is present only in archaeal and eukaryotic ribosomes (Lecompte *et al.* 2002). The archaeal version of eL19 is shorter and lacks the long C-terminal helical domain (Figure S1A) (Gabdulkhakov *et al.* 2013). Instead, it has an ∼10-aa residues-long extension after the conserved middle region. A budding yeast mutant expressing the eL19 variant mimicking the archaeal version has been shown to be viable but displays a slow growth phenotype (Kisly *et al.* 2016).

The r-protein eL24 forms the backbone of the eB13 bridge through interactions with the SSU r-protein eS6 and 18S rRNA h6, h10, and h44 (Figure 1B) (Ben-Shem *et al.* 2011). Mutational analysis of eL24 demonstrated that the interaction between eL24 and eS6 is a key component of the eB13 bridge, indicating the importance of protein–protein contacts (Kisly *et al.* 2019).

As in the case of eL19, eL24 is present in both archaeal and eukaryotic ribosomes (Lecompte *et al.* 2002). The archaeal homolog of eL24 is a short one-domain protein (Figure S1B) (Ban *et al.* 2000; Gabdulkhakov *et al.* 2013). Eukaryotic eL24 is characterized by a three-domain structure consisting of an N-terminal domain, a linker region, and a long C-terminal α-helical domain (Figure S1B) (Ben-Shem *et al.* 2011). R-protein eL24 is nonessential for yeast cell viability (Baronas-Lowell and Warner 1990; Steffen *et al.* 2012). However, using an *in vitro* assay, it was determined that ribosomes lacking eL24 have a reduced rate of poly(U) translation (Dresios *et al.* 2000). The eukaryote-specific extensions of eL24, namely the linker and α-helix, form the eB13 bridge. Analysis of yeast mutants has revealed that this bridge is important for subunit joining *in vitro* and *in vivo* (Kisly *et al.* 2019). Further analysis utilizing a cell-free translation system has demonstrated the role of the eukaryote-specific sequence of eL24 in both the initiation and elongation steps of translation. Parallel analysis of the importance of the N-terminal domain of eL24 suggests the involvement of this domain in the initiation step of translation (Kisly *et al.* 2019).

eL41 is a 25-aa residues-long, highly positively charged r-protein that forms the bridge eB14. This bridge is the only eukaryote-specific intersubunit bridge positioned at the center of the subunit interface (Figure 1) (Ben-Shem *et al.* 2011). eL41 folds into an α-helical structure and is located in a pocket formed by the 18S rRNA h25, h44, and h45 of the SSU (Figure 1B). Despite the fact that this rRNA pocket is highly conserved from bacteria to eukaryotes, no corresponding r-protein has been found in the bacterial ribosome (Lecompte *et al.* 2002). Strikingly, the gene encoding eL41 has been identified in genomes of several Euryarchaeota species, but not in Korarchaeota or Crenarchaeota species (Armache *et al.* 2013). eL41 is also one of the few nonessential r-proteins (Dresios *et al.* 2003; Steffen *et al.* 2012). Yeast cells lacking eL41 display a similar wild-type growth rate (Yu and Warner 2001). Despite this, ribosomes lacking eL41 show a decrease in peptidyltransferase activity and translational fidelity (Dresios *et al.* 2003; Meskauskas *et al.* 2003).

Taken together, the essentiality and function of eukaryote-specific domains of r-proteins in translation are still unclear, and have not been thoroughly studied. In this study, the role of bridge-forming eukaryote-specific extensions of eL19 and eL24, and the functional importance of whole r-proteins eL24 and eL41, were evaluated using *S. cerevisiae* as the eukaryotic model organism. The analysis of mutants demonstrated that eL41 plays a remarkable role in consolidating cell growth when the archaeal variant of eL19 impaired in eB12 bridge formation is expressed or the eL24 r-protein is missing. The analysis of mutants expressing the archaeal variants of eL19 and eL24 indicated that eukaryote-specific bridges eB12

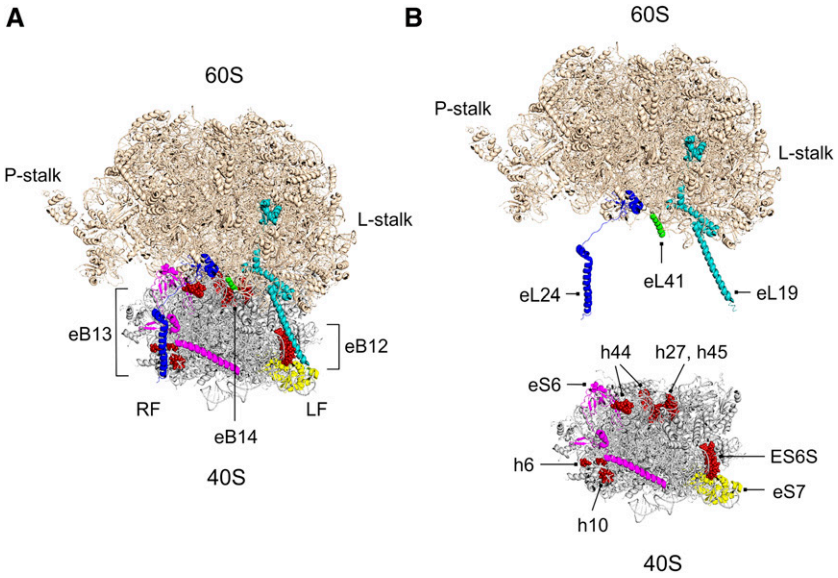

Figure 1 Structure of the *S. cerevisiae* 80S ribosome. View of the *S. cerevisiae* 80S ribosome (A) and its individual subunits (B). The large subunit (60S) is shown in wheat and the small subunit (40S) in light gray. The locations of eukaryote-specific intersubunit bridges eB12, eB13, and eB14 are indicated (A). The 60S r-proteins eL19 (teal), eL24 (dark blue), and eL41 (green)—which are the main components of eukaryote-specific intersubunit bridges eB12, eB13, and eB14—are highlighted (B). The 40S r-proteins eS6 (purple) and eS7 (yellow), helices, and expansion segment ES6S in 18S rRNA (red) forming the contacts with eL19, eL24, and eL41 are shown. The P-stalk and L-stalk are shown. The ribosome structure was generated by PyMOL (Schrodinger 2015) using coordinates from Ben-Shem *et al.* (2011). LF, left foot; RF, right foot.

and eB13 cooperatively contribute to ribosome functionality, most likely affecting the initiation step of translation. Although eukaryote-specific bridges eB12 and eB13 together with full-length eL41 are dispensable for cell growth, they play an important role in the formation of stable 80S ribosomes. Consequently, the intersubunit bridges formed by eL19, eL24, and eL41 contribute to efficient translation in eukaryotic cells.

Materials and Methods

Yeast strains and media

All *S. cerevisiae* strains used in this study were isogenic derivatives of strain S288C (Sikorski and Hieter 1989). The used strains are listed in Table S1.

Cells were grown in rich medium (YPD, 1% Bacto yeast extract, 2% Bacto peptone, and 2% glucose). For analysis of global levels of translation, cells were grown in synthetic complete medium (0.67% Bacto yeast nitrogen medium without amino acids and 2% glucose) supplemented with the appropriate amino acids and bases (Sherman 2002). Agar (2%) was added to solid media. When required, the following concentrations of antibiotics were used: 200 mg/liter geneticin, 300 mg/liter hygromycin B, and 100 mg/liter nourseothricin.

Construction of strains TYSC360 and TYSC488, and plasmids *pRS315-rpl19*$_{1–146}$ and *pRS314-rpl24*$_{1–65}$ has been described previously (Kisly *et al.* 2016, 2019). Strains TYSC517 and TYSC523 were constructed by a one-step PCR-based gene disruption method (Janke *et al.* 2004). Deletion cassettes containing *natMX6* (Hentges *et al.* 2005) were PCR amplified, and used to disrupt the *RPL41A* and *RPL41B* genes in the TYSC309 and TYSC310 strains, respectively. Yeast transformation was performed by lithium acetate/single-stranded carrier DNA/polyethylene glycol method as previously described (Knop *et al.* 1999). Strain TYSC532 was constructed by mating the TYSC517 and TYSC523 strains, followed by heterozygous diploid sporulation and tetrad dissection.

Construction of all other mutants is summarized in Figure S2. Multiple rounds of crossings were carried out. Genotypes of obtained colonies were analyzed by PCR (Lõoke *et al.* 2011).

Generation time measurements

Cultures grown overnight were diluted into fresh YPD medium. The aliquots of 150 μl cultures were incubated in a Polarstar Omega 96-well plate shaker–reader at 30°. The optical density values (OD_{600}) was measured at 7-min intervals. The generation times for at least four independent experiments with three parallel cultures were determined and presented as mean values with SD. Statistical significances of differences between strains were analyzed by Welch's ANOVA and a *post hoc* Games-Howell test at a significance level of 0.05.

Temperature-sensitivity assays

Yeast strains were grown in YPD medium at 30° to midexponential phase. The cultures were serially diluted and spotted on YPD plates. The plates were incubated for 3–8 days at different temperatures, as indicated in the figures.

Analysis of global levels of translation

Analysis of global levels of translation was performed at 30° as described previously (Kisly *et al.* 2019), with samples taken from cultures every 15 min for 2 hr. In contrast, samples from Archaea-Like (AL) AL-3Δ cultures were taken every 30 min for 4 hr. The DPM (disintegrations per minute) values divided by the OD_{600} of the samples were plotted against the corresponding time points, and the slopes of the obtained curves were calculated. The average and SD for at least four biological replicates were calculated. Statistical significances

Table 1 Analyzed mutants

Strain	Length of eL19 (aa)	Length of eL24 (aa)	Length of eL41 (aa)	Deleted regions
Wild-type	189	155	25	—
eB12Δ	146	155	25	α-helix of eL19
eB13Δ	189	65	25	α-helix and linker of eL24
eL24Δ	189	—	25	Full-length eL24
eL41Δ	189	155	—	Full-length eL41
eB12Δ eL41Δ	146	155	—	α-helix of eL19, full-length eL41
eB13Δ eL41Δ	189	65	—	α-helix and linker of eL24, full-length eL41
eL24Δ eL41Δ	189	—	—	Whole eL24, full-length eL41
AL-2Δ	146	65	25	α-helix of eL19, α-helix and linker of eL24
AL-3Δ	146	65	—	α-helix of eL19, α-helix and linker of eL24, full-length eL41

of differences between strains were analyzed by Welch's ANOVA and a *post hoc* Games-Howell test at a significance level of 0.05.

Ribosme–polysome profile analysis

Preparation of cell extracts and analysis of ribosome–polysome profiles were carried out as described earlier (Piir *et al.* 2014; Kisly *et al.* 2016, 2019). For polysome/monosome (P/M) ratio quantification, the areas under the 80S and polysome peaks were quantified by ImageJ. The average and SD for at least three biological replicates were calculated.

Preparation of salt-washed ribosomal subunits and in vitro reassociation

Salt-washed ribosomal subunits were prepared as described previously (Kisly *et al.* 2016) with modifications. Briefly, cells were lysed and 80S ribosomes were purified in high-magnesium buffer A30 [30 mM Hepes-KOH (pH 7.5), 30 mM $Mg(OAc)_2$, 100 mM KCl, 2 mM DTT, and 0.5 mM PMSF]. Next, 80S ribosome fractions were pelleted at 4° using a Ti50 rotor at $\omega^2t = 7.5 \times 10^{11}$. Dialysis of resuspended ribosomal pellets was omitted and ribosomes were immediately layered onto a 10–25% sucrose gradient in buffer B [30 mM Hepes-KOH (pH 7.5), 5 mM $Mg(OAc)_2$, 500 mM KCl, 2 mM DTT, and 0.5 mM PMSF]. Salt-washed ribosomal subunits were stored at −80° in buffer C [30 mM Hepes-KOH (pH 7.5), 5 mM $Mg(OAc)_2$, 100 mM KCl, 2 mM DTT, and 0.5 mM PMSF].

In vitro reassociation of salt-washed ribosomal subunits was performed as described previously (Kisly *et al.* 2016, 2019).

Data availability

Strains and plasmids are available upon request. Table S1 lists the *S. cerevisiae* strains used in this study. The materials and methods section in the supplemental material describes the visualization of ribosome and r-protein structures, the preparation of 80S ribosomes for mass spectrometric analysis, and liquid chromatography-tandem mass spectroscopy (LC-MS/MS) analysis. Figure S1 shows the structures of the r-proteins eL19 and eL24. Figure S2 illustrates the strategy for strain construction. Figure S3 shows the analysis of global levels of translation of eL24 mutants. Figure S4 shows the mass spectrometric analysis of ribosomes from AL mutants. Figure S5 shows the analyzed peptides originated from the r-protein eL19. Figure S6 shows the analyzed peptides originated from the r-protein eL24. Supplemental material available at figshare: https://doi.org/10.25386/genetics.9995402.

Results

During protein synthesis, the yeast ribosomal 40S and 60S subunits are associated through 12 conserved and 5 eukaryote-specific intersubunit bridges (Ben-Shem *et al.* 2011). Two of these eukaryote-specific bridges, eB12 and eB13, are located on the periphery of the ribosome (Figure 1). The main components of these bridges are eukaryote-specific extensions of the r-proteins eL19 and eL24, respectively. In contrast to the aforementioned bridges, the eukaryote-specific bridge eB14 is located in the center of the subunit interface (Figure 1). The bridge emerges due to the r-protein eL41.

eL41 ensures optimal cell growth when the eB12 bridge is impaired or r-protein eL24 is absent

Budding yeast strains impaired in eB12 or eB13 intersubunit bridge formation were constructed and thoroughly studied (Kisly *et al.* 2016, 2019). In the eB12Δ mutant, the paralogous genes encoding eL19 were deleted in the chromosome (*rpl19AΔ rpl19BΔ*), and the gene for the $eL19_{1–146}$ variant mimicking the archaeal version was ectopically expressed from a low-copy plasmid. In the eL24Δ mutant, the paralogous genes encoding eL24 were deleted (*rpl24AΔ rpl24BΔ*). In the eB13Δ mutant, the $eL24_{1–65}$ variant mimicking the archaeal version was ectopically expressed in the eL24Δ background. To analyze the importance of eL41 in cells where eB12 or eB13 bridges are compromised, or eL24 is missing, a series of mutant strains were constructed (Figure S2 and Table 1).

To study the growth characteristics of the constructed mutants in detail, temperature-sensitivity analysis by a serial dilution spot test was performed and the generation times were measured (Figure 2, A and B and Table 2). To evaluate the efficiency of translation *in vivo*, the global levels of translation were determined (Figure 2C). The incorporation of radioactive isotope-labeled amino acids into newly synthesized polypeptides was measured in exponentially growing

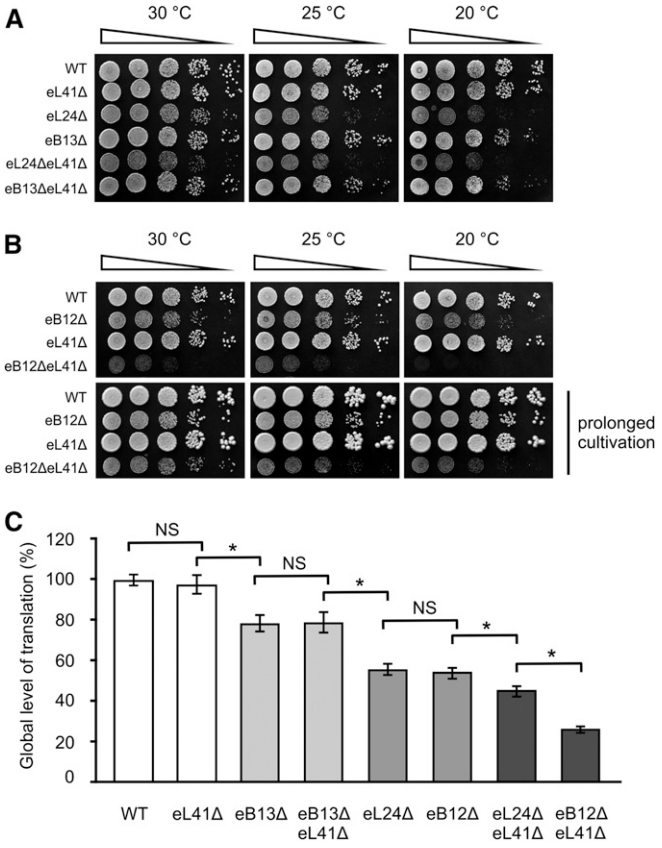

Figure 2 Phenotypic characterization of the eL19, eL24, and eL41 mutants. Growth phenotypes of the eL24 (A) and eL19 mutants (B). Serial dilutions of WT and indicated mutant strains were spotted onto rich medium. Cells were grown at the indicated temperatures for 3–5 days and for prolonged cultivation for 8 days. (C) Analysis of global levels of translation. The incorporation of radioactive isotope-labeled amino acids into newly synthesized polypeptides was measured in exponentially growing cells at 30°. Samples were taken every 15 min for 2 hr. The samples were TCA precipitated, and the incorporation of radioactive label over time was measured. The obtained values of DPM were plotted and the slope was calculated. The average slope values (mean ± SD) from at least four biological replicates are plotted. Statistical significance was determined by Welch's ANOVA and *post hoc* Games-Howell test (* $P < 0.01$; NS, $P < 0.05$). DPM, disintegrations per minute; NS, not significant; TCA, trichloroacetic acid; WT, wild-type.

yeast cells and normalized to the optical density (OD_{600}) of the cultures. Based on the impact on the growth and levels of translation, the analyzed mutants were divided into four groups.

The first group included the mutant lacking the r-protein eL41 and was thereby deficient in eB14 bridge formation (eL41Δ). This mutant exhibited wild-type growth at all analyzed temperatures (Figure 2, A and B and Table 2). This is in agreement with an earlier observation (Yu and Warner 2001). In addition, no significant difference in translation efficiency due to the loss of eL41 was observed (Figure 2C).

The second group contained mutants defective in eB13 bridge formation (eB13Δ) alone or in combination with the absence of eL41 (eB13ΔeL41Δ). These mutants displayed

Table 2 Growth of analyzed mutants

Strain[a]	Generation time (min)[b]	Fold change (mutant to WT)
WT	85.4 ± 1.9[c]	1.0
eB12Δ	128.7 ± 4.2	1.5
eB13Δ[d]	99.1 ± 3.7[e]	1.2
eL24Δ[d]	111.0 ± 3.9	1.3
eL41Δ	85.6 ± 2.3[c]	1.0
eB12Δ eL41Δ	176.1 ± 2.0	2.1
eB13Δ eL41Δ	100.8 ± 3.4[e]	1.2
eL24Δ eL41Δ	133.6 ± 2.7	1.6
AL-2Δ	224.2 ± 4.4	2.6
AL-3Δ	366.7 ± 8.8	4.3

In all cases, except those described in *c* and *e*, a statistically significant difference between strains was revealed ($P < 0.01$, Games-Howell *post hoc* test). WT, wild-type.

[a] Cells were grown in rich medium (YPD) at 30°.

[b] Generation times were calculated from at least four independent experiments in triplicate, means are shown with SD.

[c] Indicates no statistically significant difference between WT and eL41Δ strains ($P > 0.05$, Games-Howell *post hoc* test).

[d] Data from (Kisly *et al.* 2019).

[e] Indicates no statistically significant difference between eB13Δ and eB13ΔeL41Δ strains ($P > 0.05$, Games-Howell *post hoc* test).

similar growth phenotypes and had a 1.2 times longer generation times than wild-type cells (Figure 2A and Table 2). Likewise, the levels of translation in these mutants were reduced by 1.3-fold compared to wild-type cells (Figure 2C).

The mutants with a compromised eB12 bridge (eB12Δ) or lacking eL24 (eL24Δ) belonged to the third group. The absence of the eB12 bridge or full-length eL24 conferred slow growth at 30°, and the effect on growth was greater at 20° (Figure 2, A and B). These results are in agreement with previous observations (Kisly *et al.* 2016, 2019). Cells lacking eL24 displayed a 1.3-fold increase in generation time, which is consistent with published data (Baronas-Lowell and Warner 1990; Dresios *et al.* 2000; Kisly *et al.* 2019). The generation time for a mutant impaired in eB12 bridge formation was 1.5 times longer than that for wild-type cells (Table 2). As reported earlier, in cells lacking eL24, translation was reduced by 1.8-fold (Figure 2C) (Kisly *et al.* 2019). A similar reduction in translation was reported for the eB12 bridge mutant (Figure 2C).

The fourth group of mutants demonstrated synthetic sick phenotypes. First, the mutant lacking two r-proteins, eL41 and eL24 (eL24ΔeL41Δ), showed reduced growth compared to the cells without eL24 only (eL24Δ) (Figure 2A). The generation time for this mutant was 1.2 times longer than that for eL24Δ cells (Table 2). A significant, 2.2-fold reduction in the global levels of translation was detected in the eL24ΔeL41Δ mutant, indicating the genetic interaction between genes encoding the eL41 and eL24 r-proteins (Figure 2C). It is important to note that the expression of full-length eL24 restored translation in both eL24 deletion mutants analyzed (eL24Δ and eL24ΔeL41Δ) to the level observed in wild-type cells (Figure S3).

The mutant lacking r-protein eL41 and bridge eB12 (eB12ΔeL41Δ) showed severely reduced growth at 30° and

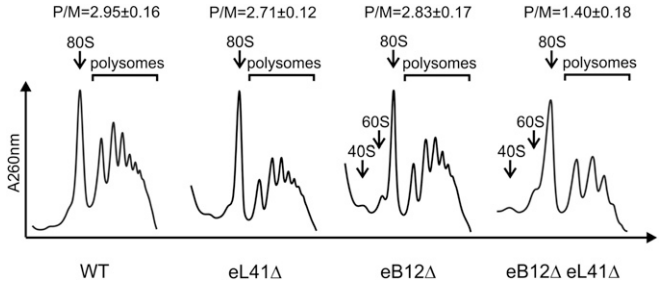

Figure 3 Analysis of ribosome–polysome profiles by sucrose density gradient centrifugation. WT cells and the indicated mutants were grown in rich medium at 30°. Whole-cell extracts were prepared from cycloheximide-treated cells and analyzed in 7–47% sucrose gradients. The absorbance at 260 nm (A260nm) was recorded. Sedimentation is from left to right. The peaks of free 60S and 40S ribosomal subunits, monosomes (80S), and polysomes are indicated. To determine the P/M ratio, the areas under the monosome (80S) and polysome peaks were quantified by ImageJ, and the P/M ratios were calculated. The average (mean ± SD) ratios of at least three biological replicates are shown. P/M, polysome/monosome; WT, wild-type.

25° (Figure 2B). The prolonged incubation of the plates gave rise to colonies at 30°, and microcolonies at 25° and 20°. eB12ΔeL41Δ displayed a generation time 1.4 times longer than cells deficient only in eB12 bridge formation and a generation time 2.1 times longer compared to wild-type cells (Table 2). A remarkable 3.7-fold reduction in translation was recorded in the eB12ΔeL41Δ mutant (Figure 2C). Thus, the absence of intersubunit bridge eB12 and r-protein eL41 caused the greatest impact on yeast cell growth and general translation. These results indicate the strong genetic interaction between r-protein eL41 and the eukaryote-specific extension of eL19.

Analysis of the ribosome–polysome profile was carried out by sedimentation of whole-cell extracts through sucrose density gradients (Figure 3). This is an effective way to analyze the translational status of the cells. In the wild-type and eL41Δ extracts, high amounts of polysomes (P/M ratio ~3), and no free 40S and 60S subunits were detected. The extracts from eB12Δ mutant cells displayed no significant changes in the P/M ratio when compared to wild-type cells. As reported earlier, in these extracts, the accumulation of free subunits was observed (Kisly *et al.* 2016). In extracts from mutants impaired in formation of the eB12 bridge and lacking eL41 (eB12ΔeL41Δ), the P/M ratio was reduced 1.7-fold. In addition, in eB12ΔeL41Δ extracts, the accumulation of free subunits was detected, which is characteristic for the eB12Δ mutant (Kisly *et al.* 2016). These results are consistent with measured generation times and global levels of translation, demonstrating once again cooperativity between eL41 and the eB12 bridge-forming region of eL19.

Altogether, these results demonstrate that eL41, and therefore the eukaryote-specific bridge eB14, becomes important when formation of bridge eB12 is impaired or eL24 is missing in cells. The mutant cells lacking two r-proteins, eL41 and eL24, displayed longer generation times and reduced levels of translation compared to cells carrying respective single r-protein mutations. In contrast, the deletion of eL41 encoding paralogous genes in eL24Δ cells expressing the archaeal variant of eL24 did not lead to any synthetic sick phenotypes. This indicates that the N-terminal domain of eL24, which is conserved in Archaea and Eukarya, is important for ribosome functionality. Indeed, a recent study suggested the role of the N-terminal domain of eL24 in the initiation step of translation (Kisly *et al.* 2019).

The mutant cells without the eB12 bridge and eL41 r-protein exhibited a more pronounced reduction in cell growth, and a decrease in global levels of translation. This demonstrates that eL41, and therefore also bridge eB14, has a strong functional interaction with bridge eB12.

The N-terminal domain of eL24 is essential when the eB12 bridge is compromised

Cells expressing the archaeal variant of eL19, which is defective in eB12 bridge formation (eB12Δ), showed slow growth at 30° and even slower growth at 20°, a 1.5 times prolonged generation time and a 1.8-fold reduction in the global levels of translation (Figure 2, B and C and Table 2). Similar phenotypes were detected for a mutant lacking the eL24 r-protein (eL24Δ) (Figure 2, A and C and Table 2). The genetic interaction between these mutations was tested using progeny of the heterologous diploid in which one copy of the A and B paralogous genes encoding eL24 were deleted in the eB12Δ background. Tetrad dissection analysis revealed that viable colonies carried either A or B, or both paralogous genes of eL24. In contrast, deletion of A and B paralogous genes simultaneously resulted in inviable spores (Figure 4A). eL24 is one of the few nonessential r-proteins. These results demonstrate that eL24 is essential for viability when the eB12 bridge is missing. To investigate the essentiality of the eB13 bridge when bridge eB12 is compromised, the progeny of the abovementioned heterologous diploid expressing the archaeal variant of eL24 ($eL24_{1–65}$) was analyzed by tetrad dissection (Figure S2C). All four spores from the single ascus were viable, and the relevant marker segregated 2:2 as expected (Figure 4A). This indicates that ribosomes lacking eukaryotic-specific bridges eB12 and eB13 retain functionality. This mutant resembles the Euryarchaeota-like ribosomes.

The spot-test analysis demonstrated a substantial reduction in the growth of the double-bridge AL mutant (AL-2Δ) at 36° and 30° compared to the single-bridge mutants (Figure 4B). The generation time for this mutant at 30° was 3.7 hr, which was 2.6 times longer than that for wild-type cells (Table 2). In addition, the AL-2Δ mutant was unable to grow at temperatures of 25° or below (Figure 4B). The observed growth defect was confirmed by measurement of the global level of translation, which was drastically reduced by 6.8-fold compared to the wild-type cells (Figure 4C).

Analysis of the ribosome–polysome profile of AL-2Δ mutant extracts demonstrated a reduced amount of 80S monosomes, and substantial accumulation of free 40S and 60S subunits compared with eB12Δ extracts (Figures 3 and 4D). In addition, a 2.2-fold reduction in the P/M ratio was

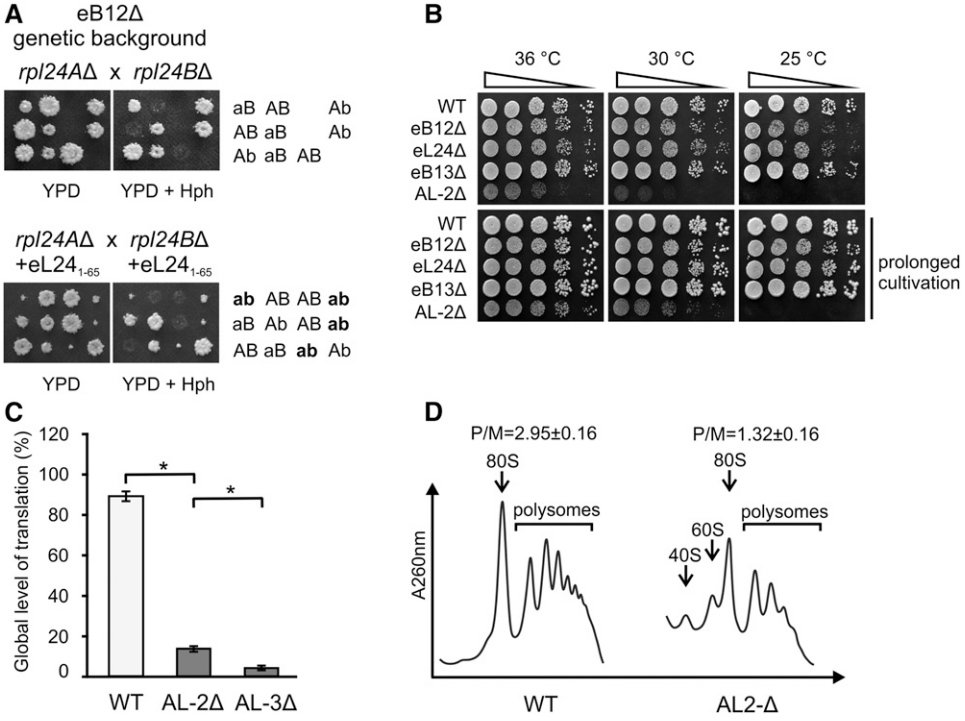

Figure 4 Phenotypic characterization of the AL-2Δ double mutant. (A) Tetrad analysis of meiotic progeny derived from eB12Δ diploid cells heterozygous for the *rpl24AΔ* and *rpl24BΔ* mutations (upper panel). Tetrad analysis of the same strain as above transformed with a plasmid expressing an archaeal variant of eL24 (eL24$_{1-65}$) (lower panel). The results from the representative tetrads for each cross are shown. Colonies were replica plated onto YPD medium supplemented with 0.3 mg/liter hygromycin B, which selects for *rpl24AΔ* and *rpl24BΔ* cells. Genotypes were conferred by PCR and are indicated on the right. The uppercase "A" or "B" indicates that the eL24 paralog A or B is present, the lowercase "a" or "b" indicates that the eL24 paralog A or B is absent. (B) Growth phenotypes of the AL-2Δ double mutant. Serial dilutions of WT and indicated mutant strains were spotted onto rich medium. The cells were grown at the indicated temperatures for 3–5 days and for prolonged cultivation for 8 days. (C) Analysis of global levels of translation of AL mutants. The incorporation of radioactive isotope-labeled amino acids into newly synthesized polypeptides was measured in exponentially growing cells at 30°. Samples were taken from WT and double-mutant (AL-2Δ) cultures every 15 min for 2 hr and from triple-mutant (AL-3Δ) cultures every 30 min for 4 hr. The samples were TCA precipitated and the incorporation of radioactive label over time was measured. The obtained values of DPM were plotted and the slope was calculated. The average slope values (mean ± SD) from at least four biological replicates are plotted. Statistical significance was determined by Welch's ANOVA and *post hoc* Games-Howell test (* $P < 0.01$). (D) Analysis of ribosome–polysome profiles by sucrose density gradient centrifugation. WT and double-mutant (AL-2Δ) cells were grown in rich medium at 30°. Whole-cell extracts were prepared from cycloheximide-treated cells and analyzed in 7–47% sucrose gradients. The absorbance at 260 nm (A260nm) was recorded. Sedimentation is from left to right. The peaks of free 60S and 40S ribosomal subunits, monosomes (80S), and polysomes are indicated. To determine the P/M ratio, the areas under the monosome (80S) and polysome peaks were quantified by ImageJ, and the P/M ratios were calculated. The average (mean ± SD) ratios of at least three biological replicates are indicated. AL, Archaea-like; DPM, disintegrations per minute; P/M, polysome/monosome; TCA, trichloroacetic acid; WT, wild-type.

detected in AL-2Δ compared to the wild-type strain. A decrease in the P/M ratio reflects a reduction in the average number of ribosomes per mRNA. As ribosome loading onto mRNA is limited by the rate of initiation, this may indicate an impaired initiation step of translation.

To analyze the importance of the eB12 and eB13 bridges in subunit joining, an *in vitro* reassociation assay using purified salt-washed ribosomal subunits was carried out. The reassociation reactions were conducted at different Mg^{2+} concentrations, and the formation of 80S was assessed by centrifugation in sucrose density gradients. As reported earlier, wild-type 60S and 40S subunits reassociate at 5 mM Mg^{2+} (Figure 5) (Kisly *et al.* 2016, 2019). However, 60S subunits carrying either the archaeal variant of eL24 or eL19 were partially associated, as manifested by intermediate particles migrating slower than 80S (Figure 5). In the absence of eB13 bridge, these intermediate particles formed at 10 mM Mg^{2+} (Kisly *et al.* 2019). In the case of a compromised eB12 bridge, intermediate particles were observed at 15 mM Mg^{2+} (Figure 5). In contrast, 60S subunits not able to form both bridges failed to reassociate regardless of the Mg^{2+} concentration. All analyzed mutant 60S subunits reassociated in the presence of saturating amounts of deacetylated transfer RNA (tRNA) at 20 mM Mg^{2+}. This indicates that these mutant 60S particles have the capability to form 80S particles when the absence of contacts between the subunits is compensated by tRNA molecules. Thus, the eB12 and eB13 bridges act cooperatively during ribosome subunit association.

Altogether, these results indicate that although eL24 is a nonessential r-protein in wild-type cells, the conserved N-terminal domain of this protein becomes essential when ribosome functionality is reduced due to a compromised eB12 bridge. The variants of eL19 and eL24 mimicking the archaeal counterparts support the viability of yeast cells. The AL ribosomes carrying these variants have reduced functionality, as can be concluded from their prolonged generation times and decreased global levels of translation. The inability to form 80S particles *in vitro* and the diminished levels of polysomes in the double-bridge mutant extracts most likely indicate obstacles at the initiation step of translation.

The loss of three eukaryote-specific bridges leads to severely reduced ribosome functionality

The bridge eB14 is positioned at the center of the subunit interface and is formed by the 60S r-protein eL41, yet its

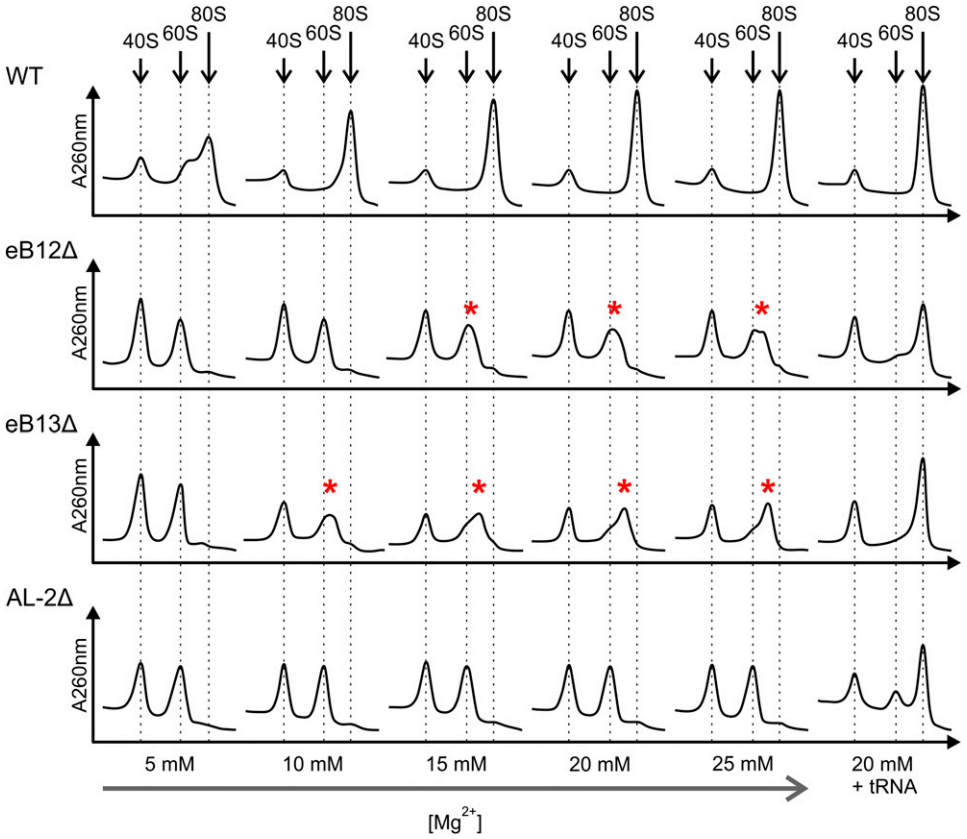

Figure 5 *In vitro* reassociation activity of 60S subunits from bridge mutants. Salt-washed 40S and 60S subunits were purified from WT, eB12Δ, and AL-2Δ strains. Two A260 units of WT 40S were mixed with two A260 units of 60S from WT or mutant strains in the presence of the indicated Mg^{2+} concentrations. Samples were incubated for 20 min at 30° and then analyzed in 10–30% sucrose gradients with the corresponding Mg^{2+} concentrations. Additionally, reactions were performed at 20 mM Mg^{2+} in the presence of a saturating concentration of deacylated tRNA (20 mM + tRNA). The reassociation activity of mutant 60S compromised in eB13 bridge formation (eB13Δ) is shown for comparison, as published previously (Kisly *et al.* 2019). Positions of 40S, 60S, and 80S particles are indicated by arrows. Intermediate particles are highlighted with red asterisks. Sedimentation is from left to right. tRNA, transfer RNA; WT, wild-type.

functional role is not known (Figure 1). Ribosomes lacking eL41 are functional; the growth and translation rates of the eL41Δ mutant are identical to those measured for the wild-type cells (Figure 2 and Table 2). In contrast, ribosomes lacking the eB12 and/or eB13 bridges have reduced functionality, which is reflected by the reduced rates of growth and translation (Figure 2 and Table 2). To test whether budding yeast ribosomes lacking the eB12 and eB13 bridges, and the eL41 r-protein retain functionality, a triple-mutant strain mimicking the AL ribosomes (AL-3Δ) was constructed. The ribosomes of Korarchaeota and Crenarchaeota lack a similar set of structural elements.

The triple-mutant strain was constructed via multiple rounds of crosses of haploid mutants followed by sporulation of the resulting diploids, tetrad dissection, and the identification of haploids carrying the right combination of alleles (Figure S2D). In the final step, a diploid heterozygous in deletions of eL24 encoding paralogous genes (eB12ΔeL41Δ background) and expressing the eL24 archaeal variant was sporulated, and tetrads were dissected. All four spores were viable in approximately in one-third of the cases. Genetic analysis of the progeny confirmed that all colonies showing severely impaired growth lacked both paralogs encoding eL24 in the genome (Figure 6A). The generation time for the triple mutant (AL-3Δ) was 6.1 hr, which is 4.3 times longer than that for wild-type cells (Table 2). The global levels of translation were substantially reduced in the AL-3Δ mutant (Figure 4C). The reduction was 25-fold when compared to wild-type cells and 3.7-fold when compared to AL-2Δ cells. The analysis of the ribosome–polysome profiles showed that, similar to the extracts of the double-bridge mutant (AL-2Δ), the removal of three eukaryotic-specific bridges caused a 2.6-fold reduction in the P/M ratio compared to the wild-type extracts (Figure 6B). In addition, this mutant exhibited a considerable accumulation of free 60S subunits and a substantial decrease in 80S monosomes.

Simultaneous expression of archaeal variants of eL19 and eL24, along with the absence of eL41, may disturb the occupancy of other r-proteins, causing defects in 40S biogenesis and a subsequent decrease in the amount of functional 80S particles. This would explain the above-described decrease in growth rate, global levels of translation, and P/M ratio. To test this possibility, the protein composition of the 80S ribosomes of the wild-type, AL-2Δ, and AL-3Δ strains was subjected to high-performance LC-MS/MS analysis as described previously (Kisly *et al.* 2019). No significant changes in the composition and ratios of r-proteins were detected in the ribosomes of bridge mutants compared to wild-type (Figure S4). In both mutants, peptides originating only from the N-terminal domain of eL24, and the N-terminal and middle domains of eL19 were detected (Figures S5 and S6). It is important to note that these peptides were present in a similar ratio when compared to identical peptides originating from wild-type ribosomes. Therefore, AL ribosomes lacking two or three bridges have compositions of r-proteins that are similar to wild-type.

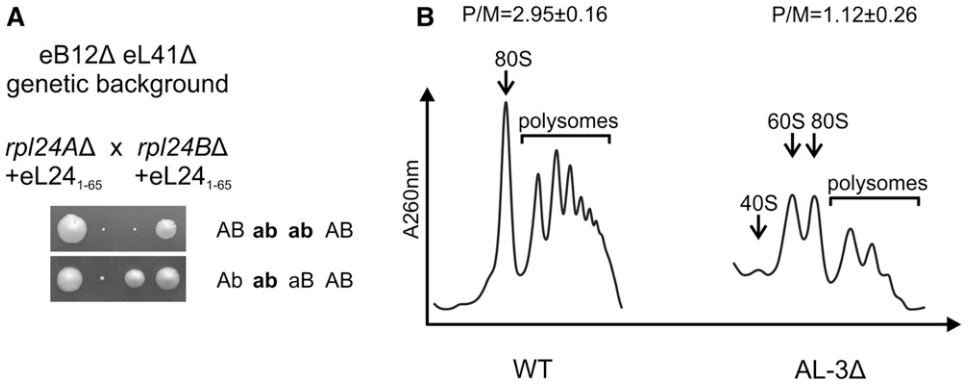

Figure 6 Phenotypic characterization of the AL-3Δ triple mutant. (A) Tetrad analysis of meiotic progeny derived from eB12ΔeL41Δ diploid cells heterozygous for the *rpl24AΔ* and *rpl24BΔ* mutations transformed with a plasmid expressing an archaeal variant of eL24 (eL24$_{1-65}$). The results from the representative tetrads are shown. Genotypes were conferred by PCR and are indicated on the right. The uppercase "A" or "B" indicates that the eL24 paralog A or B is present, the lowercase "a" or "b" indicates that the eL24 paralog A or B is absent. (B) Analysis of ribosome–polysome profiles by sucrose density gradient centrifugation. The WT cells and triple-mutant (AL-3Δ) strain were grown in rich medium at 30°. Whole-cell extracts were prepared from cycloheximide-treated cells and analyzed in 7–47% sucrose gradients. The absorbance at 260 nm (A260nm) was recorded. Sedimentation is from left to right. The peaks of free 60S and 40S ribosomal subunits, monosomes (80S), and polysomes are indicated. To determine the P/M ratio, the areas under the monosome (80S) and polysome peaks were quantified by ImageJ, and the P/M ratios were calculated. The average (mean ± SD) ratios of at least three biological replicates are indicated. AL, Archaea-like; P/M, polysome/monosome; WT, wild-type.

Together, the results indicate that AL ribosomes impaired in the formation of eB12 and eB13 bridges, and lacking eL41, are able to support cell viability. However, the functionality of such mutant ribosomes is severely compromised. The appearance of a large amount of free 60S subunits indicates defects in subunit joining. Previous studies have shown that the final maturation of pre-40S particles occurs in the cytoplasm in a complex with mature 60S subunits (Lebaron *et al.* 2012; Strunk *et al.* 2012; García-Gómez *et al.* 2014). It is possible that the shortage of the joining-competent 60S subunits leads to interference with the quality control of 40S particles and the degradation of pre-40S subunits. Alternatively, the turnover of excess free 40S subunits may prevent the accumulation of preinitiation complexes that cannot be converted to translating 80S ribosomes due to the insufficiency of functional 60S subunits, as hypothesized previously (Gregory *et al.* 2019).

In addition, the reduction in 80S ribosomes and the polysomal fraction in the triple mutant indicates that the mutant 60S subunits have a reduced ability to form 80S ribosomes. This is probably important during translation initiation because the ribosome subunit association during elongation is stabilized by the mRNA–tRNA complex.

Discussion

The r-proteins eL19, eL24, and eL41 are the main components of the ribosomal eukaryote-specific intersubunit bridges eB12, eB13, and eB14, respectively (Figure 1). In this study, the importance of the eukaryote-specific bridges eB12 and eB13, and the r-proteins eL24 and eL41, was analyzed. The functionality of ribosomes lacking different combinations of these bridges and/or r-proteins was revealed.

eL41 is incorporated into ribosomes during the late stage of cytoplasmic pre-60S maturation (Ma *et al.* 2017). The location of eL41 in the 80S ribosome has been demonstrated by several structural studies of eukaryotic ribosomes (Ben-Shem *et al.* 2011; Behrmann *et al.* 2015; Khatter *et al.* 2015). A specific quality of eL41 is that it has more contacts with the 18S rRNA of the SSU than with the 25S rRNA of the LSU (Ben-Shem *et al.* 2011). Additionally, the gene encoding eL41 is not present in all archaeal genomes. This gene has been identified in several Euryarchaeota species, but not in Korarchaeota and Crenarchaeota species (Armache *et al.* 2013). The molecular model for eL41 in the Euryarchaeota *Pyrococcus furiosus* 70S ribosome was determined indirectly using homology modeling with eL41 present in the X-ray structure of the *S. cerevisiae* 80S ribosome (Armache *et al.* 2013).

In yeast, the deletion of eL41 encoding paralogous genes is not lethal, indicating that eL41 is not essential for viability (Dresios *et al.* 2003; Steffen *et al.* 2012). Ribosomes lacking eL41 maintain functionality. The present study demonstrates that the growth and translation rates of the eL41 deletion mutant (eL41Δ) are identical to those of the wild-type cells (Figure 2, Figure 3, and Table 2). The functional importance of eL41 became evident when bridge eB12, alone or together with bridge eB13, was compromised or the full-length r-protein eL24 was absent. These results demonstrate the synergistic effect between these mutations. The mild synthetic phenotypes were observed when the deletions of both eL24-encoding genes were introduced into the eL41Δ strain. The mutant cells lacking two r-proteins, eL41 and eL24, displayed longer generation times and reduced levels of translation compared to the cells carrying respective single r-protein mutations (Figure 2 and Table 2). Second, a strong genetic interaction was observed between eL41 and the eukaryote-specific extension of eL19. Ribosomes carrying the archaeal variant of eL19 lack the eukaryote-specific extension of eL19 and are therefore impaired in eB12 bridge formation. The mutant lacking eB12 and eL41 (eB12ΔeL41Δ) showed severely reduced cell growth, and a considerable decrease in global levels of translation and polysome fraction compared to the single eB12 bridge mutant (Figure 2 and Table 2).

Third, the strongest phenotypic effects were observed when the triple mutant (AL-3Δ) was analyzed. Ribosomes in this mutant lacked the structural elements required for eB12, eB13, and eB14 bridge formation. As a result, the functionality of these ribosomes was severely compromised (Figure 6 and Table 2). Compared to the mutant lacking the eB12 and eB13 bridges simultaneously, the triple mutant displayed drastically reduced cell growth. The analysis of ribosome–polysome profiles demonstrated that 60S subunits of the triple mutant are deficient in 80S ribosome formation. Although, the function of eL41 appears to be redundant, this r-protein is important for stable ribosome association and for efficient translation.

Structural studies of bacterial, archaeal, and eukaryotic ribosomes have revealed that all ribosomes share the conserved core structure (Melnikov *et al.* 2012; Ban *et al.* 2014). During evolution, the domain-specific moieties of r-proteins or rRNAs have become attached to the ribosomes (Yusupova and Yusupov 2014). Thus, ribosomes have expanded in size upon transition from bacteria to eukaryotes. For example, a set of 35 r-proteins is found in archaeal and eukaryotic ribosomes. Most of these proteins contain conserved parts present in Archaea and Eukarya, and variable elements unique to eukaryotes (Ben-Shem *et al.* 2011). The expansion of eukaryotic ribosomes also resulted in the increase in the surface between two ribosomal subunits. As a consequence, eukaryote-specific intersubunit contacts have arisen, in which the proteins play a dominant role (Ben-Shem *et al.* 2011). The functional importance of two eukaryote-specific bridges, eB12 and eB13, have been individually studied (Kisly *et al.* 2016, 2019). In this study, two budding yeast mutants were constructed with AL ribosomes. Cells expressing the archaeal variants of eL19 and eL24 (mutant AL-2Δ) have ribosomes defective in eB12 and eB13 bridge formation. These ribosomes are reminiscent of Euryarchaeal ribosomes. In the triple mutant (AL-3Δ), ribosomes are not able to form bridges eB12 and eB13, and lack the eL41 r-protein. Ribosomes in this mutant are similar to Korarchaeota and Crenarchaeota ribosomes. The phenotypic analysis of these AL mutants demonstrated that the formation of functional 80S ribosomes during translation initiation is severely hampered. In turn, this causes a drastic reduction in cell growth and global levels of translation. It is intriguing that despite several attempts, it was not possible to isolate 70S ribosomes from the archaeal species *Methanococcus igneus*, *Thermococcus kodakaraensis*, and *Methanothermobacter thermautotrophicus*. Instead, only free ribosomal subunits appeared on the sucrose gradients (Greber *et al.* 2012; Armache *et al.* 2013). Euryarchaeal 70S ribosomes lack intersubunit bridges such as eB12 and eB13, which is likely the reason for weak ribosome subunit association. Thus, during evolution, after the split of the eukaryotic and archaeal linages, the eukaryotic ribosomes acquired additional protein and RNA sequences, and developed more sophisticated structures. The eukaryote-specific intersubunit bridges serve as stabilizing elements for this complex structure. A recent study on the structural diversity of ribosomal core proteins demonstrated that nonglobular extensions of r-proteins carry most of the structural variations (Melnikov *et al.* 2018). It was proposed that this structural variation appears to reflect the functional specialization of core r-proteins. The results of the present study suggest that the connection between structural variation and specialization is characteristic not only to the core r-proteins, but also to other r-proteins. Thus, the eukaryote-specific extensions of r-proteins that participate in the formation of intersubunit bridges may facilitate translation and thus provide a growth advantage for eukaryotes.

Acknowledgments

We thank all members of the Chair of Molecular Biology, especially Aivar Liiv, Margus Leppik, Silva Lilleorg, Kaspar Reier, and Pavel Volõnkin for their support and for helpful discussions. We also thank Sergo Kasvandik for help with mass spectrometric analysis. This work was supported by a grant from the Estonian Ministry of Education and Research to J.R. (Estonian Research Council Institutional Research Funding Project number IUT20-21).

Literature Cited

Anger, A. M., J. P. Armache, O. Berninghausen, M. Habeck, M. Subklewe *et al.*, 2013 Structures of the human and Drosophila 80S ribosome. Nature 497: 80–85. https://doi.org/10.1038/nature12104

Armache, J. P., A. M. Anger, V. Marquez, S. Franckenberg, T. Frohlich *et al.*, 2013 Promiscuous behaviour of archaeal ribosomal proteins: implications for eukaryotic ribosome evolution. Nucleic Acids Res. 41: 1284–1293. https://doi.org/10.1093/nar/gks1259

Ban, N., P. Nissen, J. Hansen, P. B. Moore, and T. A. Steitz, 2000 The complete atomic structure of the large ribosomal subunit at 2.4 A resolution. Science 289: 905–920. https://doi.org/10.1126/science.289.5481.905

Ban, N., R. Beckmann, J. H. Cate, J. D. Dinman, F. Dragon *et al.*, 2014 A new system for naming ribosomal proteins. Curr. Opin. Struct. Biol. 24: 165–169. https://doi.org/10.1016/j.sbi.2014.01.002

Baronas-Lowell, D. M., and J. R. Warner, 1990 Ribosomal protein L30 is dispensable in the yeast Saccharomyces cerevisiae. Mol. Cell. Biol. 10: 5235–5243. https://doi.org/10.1128/MCB.10.10.5235

Behrmann, E., J. Loerke, T. V. Budkevich, K. Yamamoto, A. Schmidt *et al.*, 2015 Structural snapshots of actively translating human ribosomes. Cell 161: 845–857. https://doi.org/10.1016/j.cell.2015.03.052

Ben-Shem, A., N. Garreau de Loubresse, S. Melnikov, L. Jenner, G. Yusupova *et al.*, 2011 The structure of the eukaryotic ribosome at 3.0 A resolution. Science 334: 1524–1529. https://doi.org/10.1126/science.1212642

Dresios, J., I. L. Derkatch, S. W. Liebman, and D. Synetos, 2000 Yeast ribosomal protein L24 affects the kinetics of protein synthesis and ribosomal protein L39 improves translational accuracy, while mutants lacking both remain viable. Biochemistry 39: 7236–7244. https://doi.org/10.1021/bi9925266

Dresios, J., P. Panopoulos, K. Suzuki, and D. Synetos, 2003 A dispensable yeast ribosomal protein optimizes peptidyltransferase activity and affects translocation. J. Biol. Chem. 278: 3314–3322. https://doi.org/10.1074/jbc.M207533200

Gabdulkhakov, A., S. Nikonov, and M. Garber, 2013 Revisiting the Haloarcula marismortui 50S ribosomal subunit model. Acta Crystallogr. D Biol. Crystallogr. 69: 997–1004. https://doi.org/10.1107/S0907444913004745

García-Gómez, J. J., A. Fernández-Pevida, S. Lebaron, I. V. Rosado, D. Tollervey *et al*., 2014 Final pre-40S maturation depends on the functional integrity of the 60S subunit ribosomal protein L3. PLoS Genet. 10: e1004205. https://doi.org/10.1371/journal.pgen.1004205

Greber, B. J., D. Boehringer, V. Godinic-Mikulcic, A. Crnkovic, M. Ibba *et al*., 2012 Cryo-EM structure of the archaeal 50S ribosomal subunit in complex with initiation factor 6 and implications for ribosome evolution. J. Mol. Biol. 418: 145–160. https://doi.org/10.1016/j.jmb.2012.01.018

Gregory, B., N. Rahman, A. Bommakanti, M. Shamsuzzaman, M. Thapa *et al.*, 2019 The small and large ribosomal subunits depend on each other for stability and accumulation. Life Sci. Alliance 2: e201800150 (erratum: Life Sci. Alliance 2: e201900508).

Hentges, P., B. Van Driessche, L. Tafforeau, J. Vandenhaute, and A. M. Carr, 2005 Three novel antibiotic marker cassettes for gene disruption and marker switching in Schizosaccharomyces pombe. Yeast 22: 1013–1019. https://doi.org/10.1002/yea.1291

Janke, C., M. M. Magiera, N. Rathfelder, C. Taxis, S. Reber *et al*., 2004 A versatile toolbox for PCR-based tagging of yeast genes: new fluorescent proteins, more markers and promoter substitution cassettes. Yeast 21: 947–962. https://doi.org/10.1002/yea.1142

Khatter, H., A. G. Myasnikov, S. K. Natchiar, and B. P. Klaholz, 2015 Structure of the human 80S ribosome. Nature 520: 640–645. https://doi.org/10.1038/nature14427

Kisly, I., S. P. Gulay, U. Maeorg, J. D. Dinman, J. Remme *et al*., 2016 The functional role of eL19 and eB12 intersubunit bridge in the eukaryotic ribosome. J. Mol. Biol. 428: 2203–2216. https://doi.org/10.1016/j.jmb.2016.03.023

Kisly, I., J. Remme, and T. Tamm, 2019 Ribosomal protein eL24, involved in two intersubunit bridges, stimulates translation initiation and elongation. Nucleic Acids Res. 47: 406–420. https://doi.org/10.1093/nar/gky1083

Klinge, S., F. Voigts-Hoffmann, M. Leibundgut, and N. Ban, 2012 Atomic structures of the eukaryotic ribosome. Trends Biochem. Sci. 37: 189–198. https://doi.org/10.1016/j.tibs.2012.02.007

Knop, M., K. Siegers, G. Pereira, W. Zachariae, B. Winsor *et al*., 1999 Epitope tagging of yeast genes using a PCR-based strategy: more tags and improved practical routines. Yeast 15: 963–972. https://doi.org/10.1002/(SICI)1097-0061(199907)15:10B<963::AID-YEA399>3.0.CO;2-W

Lebaron, S., C. Schneider, R. W. van Nues, A. Swiatkowska, D. Walsh *et al*., 2012 Proofreading of pre-40S ribosome maturation by a translation initiation factor and 60S subunits. Nat. Struct. Mol. Biol. 19: 744–753. https://doi.org/10.1038/nsmb.2308

Lecompte, O., R. Ripp, J. C. Thierry, D. Moras, and O. Poch, 2002 Comparative analysis of ribosomal proteins in complete genomes: an example of reductive evolution at the domain scale. Nucleic Acids Res. 30: 5382–5390. https://doi.org/10.1093/nar/gkf693

Lõoke, M., K. Kristjuhan, and A. Kristjuhan, 2011 Extraction of genomic DNA from yeasts for PCR-based applications. Biotechniques 50: 325–328. https://doi.org/10.2144/000113672

Ma, C., S. Wu, N. Li, Y. Chen, K. Yan *et al*., 2017 Structural snapshot of cytoplasmic pre-60S ribosomal particles bound by Nmd3, Lsg1, Tif6 and Reh1. Nat. Struct. Mol. Biol. 24: 214–220. https://doi.org/10.1038/nsmb.3364

Melnikov, S., A. Ben-Shem, N. Garreau de Loubresse, L. Jenner, G. Yusupova *et al*., 2012 One core, two shells: bacterial and eukaryotic ribosomes. Nat. Struct. Mol. Biol. 19: 560–567. https://doi.org/10.1038/nsmb.2313

Melnikov, S., K. Manakongtreecheep, and D. Soll, 2018 Revising the structural diversity of ribosomal proteins across the three domains of life. Mol. Biol. Evol. 35: 1588–1598. https://doi.org/10.1093/molbev/msy021

Meskauskas, A., J. W. Harger, K. L. Jacobs, and J. D. Dinman, 2003 Decreased peptidyltransferase activity correlates with increased programmed -1 ribosomal frameshifting and viral maintenance defects in the yeast Saccharomyces cerevisiae. RNA 9: 982–992. https://doi.org/10.1261/rna.2165803

Piir, K., T. Tamm, I. Kisly, T. Tammsalu, and J. Remme, 2014 Stepwise splitting of ribosomal proteins from yeast ribosomes by LiCl. PLoS One 9: e101561. https://doi.org/10.1371/journal.pone.0101561

Planta, R. J., and W. H. Mager, 1998 The list of cytoplasmic ribosomal proteins of Saccharomyces cerevisiae. Yeast 14: 471–477. https://doi.org/10.1002/(SICI)1097-0061(19980330)14:5<471::AID-YEA241>3.0.CO;2-U

Pöll, G., T. Braun, J. Jakovljevic, A. Neueder, S. Jakob *et al*., 2009 rRNA maturation in yeast cells depleted of large ribosomal subunit proteins. PLoS One 4: e8249. https://doi.org/10.1371/journal.pone.0008249

Schrodinger, LLC, 2015 The PyMOL Molecular Graphics System, Version 1.5.0.5, Available at: https://pymol.org

Sherman, F., 2002 Getting started with yeast. Methods Enzymol. 350: 3–41. https://doi.org/10.1016/S0076-6879(02)50954-X

Sikorski, R. S., and P. Hieter, 1989 A system of shuttle vectors and yeast host strains designed for efficient manipulation of DNA in Saccharomyces cerevisiae. Genetics 122: 19–27.

Steffen, K. K., M. A. McCormick, K. M. Pham, V. L. MacKay, J. R. Delaney *et al*., 2012 Ribosome deficiency protects against ER stress in Saccharomyces cerevisiae. Genetics 191: 107–118. https://doi.org/10.1534/genetics.111.136549

Strunk, B. S., M. N. Novak, C. L. Young, and K. Karbstein, 2012 A translation-like cycle is a quality control checkpoint for maturing 40S ribosome subunits. Cell 150: 111–121. https://doi.org/10.1016/j.cell.2012.04.044

Yu, X., and J. R. Warner, 2001 Expression of a micro-protein. J. Biol. Chem. 276: 33821–33825. https://doi.org/10.1074/jbc.M103772200

Yusupov, M. M., G. Z. Yusupova, A. Baucom, K. Lieberman, T. N. Earnest *et al*., 2001 Crystal structure of the ribosome at 5.5 A resolution. Science 292: 883–896. https://doi.org/10.1126/science.1060089

Yusupova, G., and M. Yusupov, 2014 High-resolution structure of the eukaryotic 80S ribosome. Annu. Rev. Biochem. 83: 467–486. https://doi.org/10.1146/annurev-biochem-060713-035445

Communicating editor: A. Hinnebusch